JPE 16-5-17

http://dx.doi.org/10.6113/JPE.2016.16.5.1781
ISSN(Print): 1598-2092 / ISSN(Online): 2093-4718

Coordination Control of Multiple Electrical Excited Synchronous Motors and Its Application in High-Power Metal-Rolling Systems

Jing Shang[†,**], Xiaohong Nian[*], and Yong Liu[**]

[†,*]School of Information Science and Engineering, Central South University, Changsha, China
[**]CRRC Zhuzhou Institute Co., Ltd., Zhuzhou, China

Abstract

This study focuses on the coordination control problem of multiple electrical excited synchronous motor systems. A robust coordination controller is designed on the basis of cross coupling and an interval matrix. The proposed control strategy can deal with load uncertainty. In addition, the proposed control strategy is applied to a high-power metal-rolling system. Simulation and experiment results demonstrate that the proposed control strategy achieves good dynamic and static performance. It also shows better coordination performance than traditional proportional–integral controllers.

Key words: Coordination control, Electrical excited synchronous motor, Interval matrix, Inverter, Metal-rolling

I. INTRODUCTION

The use of coupling multi-motor systems (CMMSs) in industry, agriculture, and transportation is steadily increasing. Coupling multi-motor systems require good coordination to achieve good production quality, reduce contouring errors, and improve the operation security of systems. In recent decades, many coordination control strategies have been designed for multi-motor systems. The work in [1] developed a chaotic speed synchronization controller for multiple induction motors using stator flux regulation. In [2], a cross-coupled intelligent complementary sliding mode control for dual linear motor servo systems was proposed on the basis of a Takagi–Sugeno–Kang-type fuzzy neural network estimator. The work in [3] simplified the control structure by presenting an adjacent cross-coupling control architecture incorporating sliding mode control for multiple induction motors. In [4], precision motion control was achieved by combining individual axis iterative learning control (ILC) and cross-coupled ILC into a single control input. To track different desired trajectories, the work in [5] exploited a generalized synchronization controller for multi-axis motion systems by integrating cross-coupling technology into optimal control architecture. In [6], an optimal synchronization for high-precision motion system was designed by introducing coupling and synchronization factors into the synchronization error. Many other control strategies have been adopted in this field, and they include adaptive control [7]-[9], fuzzy control [10], [11], electronic line-shafting control [12], [13], robust control [14]-[19], neural network control [20], gain-scheduled control [21], and model-free control [22].

Compared with asynchronous induction motors, electrical excited synchronous motors (EESMs) achieve higher efficiency, power density, and so on. EESMs are applied in many fields, such as in mine-hoisting, metallurgy, metal-rolling, and marine propulsion, particularly in the field of high-power industrial drives. The present work explores the coordination control of multiple EESMs.

The dynamic model of driving devices is seldom or never considered in CMMSs when controllers are designed [2], [5], [12], [13], [16]–[21]. If the dynamic model of a driving device is fully considered, the dynamic performance of a system significantly improves. Therefore, a multiple externally excited synchronous motor system is studied in the current work. A dynamic model of an EESM is considered to improve the dynamic performance of the studied system.

Manuscript received Jan. 19, 2016; accepted May 22, 2016
Recommended for publication by Associate Editor Jung-Ik Ha.
[†]Corresponding author: shangjing@csrzic.com
Tel: +86-0733-28494371, Fax: +86-0733-28494371, Central South University
[*]School of Information Science and Eng., Central South Univ., China
[**]CRRC Zhuzhou Institute Co., Ltd., China

When a parameter is uncertain or changes with time, an interval matrix is normally introduced [23], [24]. Confined by supply voltage and protection equipment, the current and speed of an EESM are limited to a rated range. Although many coordination control strategies have been developed, cross coupling remains widely adopted in coordination controller design [2]. Interval matrix and the cross-coupling concept are introduced to design the controller of a multiple EESM system.

This paper is organized as follows. The mathematical model of a multiple EESM system is presented in Section II. The coordination controller design is presented in Section III. The application of the proposed design in a high-power metal-rolling system is described in Section IV. Conclusions are given in Section V.

II. MATHEMATICAL MODEL

The following notations are used throughout the paper. I is the identity matrix with an appropriate dimension, and e_i is the ith column of matrix I. 0_{ij} denotes the zero matrix with $i \times j$ dimensions.

If matrices $A^m = [a_{ij}^m]_{n\times n}$ and $A^M = [a_{ij}^M]_{n\times n}$ satisfy $a_{ij}^m \le a_{ij}^M$ for all $1 \le i \le n$ and $1 \le j \le n$, then $[A^m \quad A^M] = \{[a_{ij}] : a_{ij}^m \le a_{ij} \le a_{ij}^M, 1 \le i, j \le n\}$ can be defined. Assume $A \in R^{n\times n}$ and $A \in [A^m \quad A^M]$; then, A is an interval matrix.

Lemma 1 [29]. For a given interval matrix $A \in [A^m \quad A^M]$ and $A \in R^{n\times n}$, A can be rewritten as

$$A = A_0 + E\Delta G, \Delta \in \Delta^*.$$

where $A_0 = \frac{1}{2}(A^M + A^m), H = [h_{ij}]_{n\times n} = \frac{1}{2}(A^M - A^m)$. The elements in matrices A^m and A^M consist of the lower bound and upper bound of the elements in matrix A, respectively. Each element in matrix H is nonnegative.

$$\begin{aligned}\Delta^* &= \{\Delta \in R^{n^2\times n^2} \mid \Delta \\ &= diag\{\chi_{11} \ \cdots \ \chi_{1n} \ \cdots \ \chi_{n1} \ \cdots \ \chi_{nn}\}, \\ &\quad |\chi_{ij}| \le 1, i, j = 1, \cdots, n\},\end{aligned}$$

$$E = \left[\sqrt{h_{11}}e_1 \ \cdots \ \sqrt{h_{1n}}e_1 \ \cdots \ \sqrt{h_{n1}}e_n \ \cdots \ \sqrt{h_{nn}}e_n\right]$$

$$G = \left[\sqrt{h_{11}}e_1 \ \cdots \ \sqrt{h_{1n}}e_n \ \cdots \ \sqrt{h_{n1}}e_1 \ \cdots \ \sqrt{h_{nn}}e_n\right]^T_{n\times n^2}.$$

Lemma 2 [24]. For any given interval matrix $A \in [A^m \quad A^M]$, matrix $A_0 = \frac{1}{2}(A^M + A^m)$, and $H = [h_{ij}]_{n\times n} = \frac{1}{2}(A^M - A^m)$, A can be written as $A = A_0 + \sum_{i,j=1}^{n} e_i f_{ij} e_j^T$, where $|f_{ij}| \le h_{ij}$.

Lemma 3 [30] For any scalar $\varepsilon > 0$ and real matrices X and Y with appropriate dimensions, the following inequality is established.

$$X^T Y + Y^T X \le \frac{X^T X}{\varepsilon} + \varepsilon Y^T Y.$$

According to [31], the mathematical model of EESMs can be described as follows.

$$\begin{cases}\dfrac{di_f}{dt} = \dfrac{L_{md}R_s}{\sigma L_{sd}L_f} i_{sd} - \dfrac{L_{md}L_{sq}}{\sigma L_{sd}L_f}\omega i_{sq} - \dfrac{R_f}{\sigma L_f} I_f - \dfrac{L_{md}}{\sigma L_{sd}L_f}u_{sd} + \dfrac{L_{md}}{\sigma L_{sd}L_f}u_f, \\ \dfrac{di_{sd}}{dt} = -\dfrac{R_s}{\sigma L_{sd}} i_{sd} + \dfrac{L_{sq}}{\sigma L_{sd}}\omega i_{sq} + \dfrac{L_{md}R_f}{\sigma L_{sd}L_f} I_f + \dfrac{1}{\sigma L_{sd}}u_{sd} - \dfrac{L_{md}}{\sigma L_{sd}L_f}u_f, \\ \dfrac{di_{sq}}{dt} = -\dfrac{L_{sdi}}{L_{sqi}}\omega i_{sd} - \dfrac{R_s}{L_{sq}} i_{sq} - \dfrac{L_{md}}{L_{sq}}\omega I_f + \dfrac{1}{L_{sq}}u_{sq}, \\ \dfrac{d\omega}{dt} = \dfrac{n_p^2}{J}(L_{md}I_f i_{sq} - (L_{md} - L_{mq})i_{sd}i_{sq}) - \dfrac{n_p}{J}T_l - \dfrac{n_p B}{J}\omega,\end{cases} \tag{1}$$

where L_{sd} and L_{sq} are the d- and q-axis self-inductions, respectively; L_{md} and L_{mq} are the d- and q-axis inductances, respectively; L_f is the excitation winding self-induction; $\sigma = 1 - \frac{L_{md}^2}{L_{sd}L_f}$ is the leakage coefficient; R_f is the excitation winding resistance; R_s is the stator resistance; n_p is the number of pole pairs; B is the frictional coefficient; J is the moment inertia; i_f is the excitation current; i_{sd} and i_{sq} are the d- and q-axis currents, respectively; ω is the rotor angular speed; u_f is the excitation voltage; u_{sd} and u_{sq} are the d- and q-axis input voltages, respectively; and T_l is the load torque.

Remark 1. *Damper winding is not considered in the aforementioned model. That is, damping winding is assumed to be constant in this work.*

If model error and disturbance are considered, the ith subsystem (i.e., motor i) is described as

$$\begin{cases}\dfrac{di_{fi}}{dt} = \dfrac{L_{mdi}R_{si}}{\sigma_i L_{sdi}L_{fi}} i_{sdi} - \dfrac{L_{mdi}L_{sqi}}{\sigma_i L_{sdi}L_{fi}}\omega_i i_{sqi} - \dfrac{R_{fi}}{\sigma_i L_{fi}} i_{fi} \\ \qquad - \dfrac{L_{mdi}}{\sigma_i L_{sdi}L_{fi}}u_{sdi} + \dfrac{L_{mdi}}{\sigma_i L_{sdi}L_{fi}}u_{fi} + d_{fi}, \\ \dfrac{di_{sdi}}{dt} = -\dfrac{R_{si}}{\sigma_i L_{sdi}} i_{sdi} + \dfrac{L_{sqi}}{\sigma_i L_{sdi}}\omega_i i_{sqi} + \dfrac{L_{mdi}R_{fi}}{\sigma_i L_{sdi}L_{fi}} i_{fi} \\ \qquad + \dfrac{1}{\sigma_i L_{sdi}}u_{sdi} - \dfrac{L_{mdi}}{\sigma_i L_{sdi}L_{fi}}u_{fi} + d_{di}, \\ \dfrac{di_{sqi}}{dt} = -\dfrac{L_{sdi}}{L_{sqi}}\omega_i i_{sdi} - \dfrac{R_{si}}{L_{sqi}} i_{sqi} - \dfrac{L_{mdi}}{L_{sqi}}\omega_i i_{fi} + \dfrac{1}{L_{sqi}}u_{sqi} + d_{qi}, \\ \dfrac{d\omega_i}{dt} = \dfrac{n_{pi}^2}{J_i}(L_{mdi}I_{fi}i_{sqi} - (L_{mdi} - L_{mqi})i_{sdi}i_{sqi}) \\ \qquad - \dfrac{n_{pi}}{J_i}T_{li} - \dfrac{n_{pi}B_i}{J_i}\omega_i + d_{\omega i},\end{cases} \tag{2}$$

where L_{sdi} and L_{sqi} are the d- and q-axis self-inductions of motor i, respectively; L_{mdi} and L_{mqi} are the d- and q-axis inductances of motor i, respectively; L_{fi} is the excitation winding self-induction of motor i; $\sigma_i = 1 - \frac{L_{mdi}^2}{L_{sdi}L_{fi}}$ is the leakage coefficient of motor i; R_{fi} is the excitation winding resistance of motor i; R_{si} is the stator resistance of motor i; n_{pi} is the number of pole pairs of motor i; B_i is the frictional coefficient of motor i; J_i is the moment inertia of motor i; i_{fi} is the excitation current of motor i; i_{sdi} and i_{sqi} are the d- and q-axis currents of motor i, respectively; ω_i is the rotor angular speed of motor i; u_{fi} is the excitation voltage of motor i; u_{sdi} and u_{sqi} are the d- and q-axis input voltages of motor i, respectively; T_{li} is the load torque of motor i; d_{fi}, d_{di}, d_{qi}, and $d_{\omega i}$ present the model error and/or disturbance; and subscript $i = 1, \cdots, n$.

As the changes in disturbance and load are usually slow, the following condition is often satisfied, similar to that in [25], [26].

$$\frac{dd_{fi}}{dt} \approx 0, \frac{dd_{di}}{dt} \approx 0, \frac{dd_{qi}}{dt} \approx 0, \frac{dd_{\omega i}}{dt} \approx 0, \frac{dT_{li}}{dt} \approx 0 \tag{3}$$

The current and speed of each EESM are constrained by supply power, rated parameter, protection equipment, and so on. Thus, they are restricted to a certain range or "rated" range. Hence, the following assumptions are reasonable.

$$i_{fi}^m \le i_{fi} \le i_{fi}^M, i_{sdi}^m \le i_{sdi} \le i_{sdi}^M, i_{sqi}^m \le i_{sqi} \le i_{sqi}^M, \omega_i^m \le \omega_i \le \omega_i^M \tag{4}$$

The state variables and control inputs of subsystem i are chosen as

$$\begin{aligned} X_i &= \left[x_j^i\right]_{5\times 1} = [i_{fi} i_{sdi} \int_0^t i_{sdi} ds \;\; i_{sqi} \;\; \omega_i - \omega_i^* \int_0^t (\omega_i - \omega_i^*) ds]^T, \\ U_i &= \left[u_j^i\right]_{3\times 1} = [u_{fi} \;\; u_{di} \;\; u_{qi}]^T \end{aligned} \tag{5}$$

where ω_i^* is the desired speed of the ith subsystem and is a constant.

Tracking error is defined as

$$\Delta\omega_i = \omega_i^* - \omega_i \tag{6}$$

In coordination control, the desired speed of each motor may be different. ω_i^* may not equal ω_j^* when $i \ne j$. Scalars ω_i^* and ω_j^* should be introduced to describe the coordination error of the *ith* motor and *jth* motor. The coordination error between the *ith* motor and the *jth* motor can be defined as

$$\Delta\omega_{ij} = \omega_j^* \omega_i - \omega_i^* \omega_j \tag{7}$$

The mathematical model of subsystem i is described as follows , according to (2) and (5).

$$X_i = A_i X_i + B_i U_i + f_i(x_j^i) \tag{8}$$

where

$$A_i = \begin{bmatrix} -\frac{R_{fi}}{\sigma_i L_{fi}} & \frac{L_{mdi}L_{sqi}R_{si}}{\sigma_i L_{sdi} L_{fi}} & 0 & 0 & 0 & 0 \\ \frac{L_{mdi}R_{fi}}{\sigma_i L_{sdi} L_{fi}} & -\frac{R_{si}}{\sigma_i L_{sdi}} & 0 & 0 & 0 & 0 \\ 0 & 1 & 0 & 0 & 0 & 0 \\ 0 & 0 & 0 & -\frac{R_{si}}{L_{sqi}} & 0 & 0 \\ 0 & 0 & 0 & 0 & -\frac{n_{pi}B_i}{J_i} & 0 \\ 0 & 0 & 0 & 0 & 1 & 0 \end{bmatrix},$$

$$B_i = \begin{bmatrix} \frac{1}{\sigma_i L_{fi}} & -\frac{L_{mdi}}{\sigma_i L_{sdi} L_{fi}} & 0 & 0 & 0 & 0 \\ -\frac{L_{mdi}}{\sigma_i L_{sdi} L_{fi}} & \frac{1}{\sigma_i L_{sdi}} & 0 & 0 & 0 & 0 \\ 0 & 0 & 0 & \frac{1}{L_{sdi}} & 0 & 0 \end{bmatrix}^T,$$

$$f_i(x_j^i) = \begin{bmatrix} -\frac{L_{mdi}L_{sqi}}{\sigma_i L_{sdi} L_{si}} x_4^i (x_5^i + \omega^*) + d_{fi} \\ \frac{L_{sqi}}{\sigma_i L_{sdi}} x_4^i (x_5^i + \omega^*) + d_{di} \\ 0 \\ -(\frac{L_{mdi}}{L_{sqi}} x_1^i + \frac{L_{sdi}}{L_{sqi}} x_2^i)(x_5^i + \omega^*) + d_{qi} \\ f_i^{15} \\ 0 \end{bmatrix},$$

$$f_i^{15} = \frac{n_{pi}^2}{J_i}(L_{mdi} x_1^i x_4^i + (L_{mdi} - L_{mqi}) x_2^i x_4^i) - \frac{n_{pi}}{J_i} T_{li} - \frac{B_i}{J_i} \omega_i^* + d_{\omega i}$$

According to (8), the model of a multiple three-level EESM system is expressed as

$$X = AX + BU + F(x_j^i) \tag{9}$$

where

$$X = \left[X_1 \;\; \cdots \;\; X_i \;\; \cdots \;\; X_n\right]^T,$$

$$U = \left[U_1 \;\; \cdots \;\; U_i \;\; \cdots \;\; U_n\right]^T,$$

$$A = diag\{A_1 \;\; \cdots \;\; A_i \;\; \cdots \;\; A_n\},$$

$$B = diag\{B_1 \;\; \cdots \;\; B_i \;\; \cdots \;\; B_n\},$$

$$F(x_j^i) = diag\{f_1(x_j^1) \;\; \cdots \;\; f_i(x_j^i) \;\; \cdots \;\; f_n(x_j^n)\}.$$

III. Coordination Controller Design

A coordination controller should be designed to ensure that the system achieves a good coordination performance and that each motor can track its own desired speed. The control structure of the system is described in Fig. 1.

The auxiliary matrices are defined as

$$Q_0 = diag\{Q_1^0 \;\; \cdots \;\; Q_i^0 \;\; \cdots \;\; Q_n^0\},$$

$$\Delta Q = [\Delta q_{ij}]_{5n\times 5n} = diag\{\Delta Q_1 \;\; \cdots \;\; \Delta Q_i \;\; \cdots \;\; \Delta Q_n\},$$

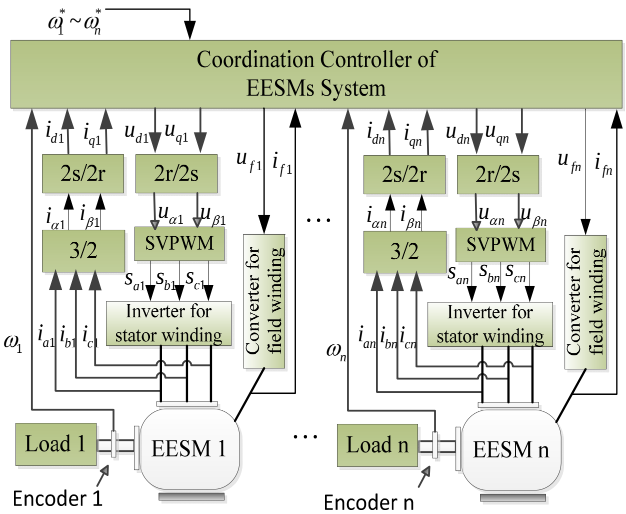

Fig. 1. Control structure of the system.

$$E_1=\left[\sqrt{\Delta q_{11}}e_1 \ \cdots \ \sqrt{\Delta q_{16n}}e_1 \ \cdots \ \sqrt{\Delta q_{6n1}}e_{5n} \ \cdots \ \sqrt{\Delta q_{6n6n}}e_{6n}\right]_{6n\times(6n)^2},$$

$$G_1=\left[\sqrt{\Delta q_{11}}e_1 \ \cdots \ \sqrt{\Delta q_{16n}}e_{6n} \ \cdots \ \sqrt{\Delta q_{6n1}}e_1 \ \cdots \ \sqrt{\Delta q_{6n6n}}e_{6n}\right]^T_{(6n)^2\times 6n}.$$

where,

$$Q_i^0=[q_{ij}^{i0}]_{6\times6}=\begin{bmatrix} Q_{i11}^0 & \dfrac{L_{sqi}}{2\sigma_i L_{sdi}}Q_{i12}^0 \\ Q_{i21}^0 & Q_{i22}^0 \end{bmatrix},$$

$$Q_{i11}^0=0_{3\times3},$$

$$Q_{i12}^0=\begin{bmatrix} -\dfrac{L_{mdi}}{L_{si}}(\omega_i^M+\omega_i^m) & -\dfrac{L_{mdi}}{L_{si}}(i_{sqi}^M+i_{sqi}^m) & 0 \\ -(\omega_i^M+\omega_i^m) & -(i_{sqi}^M+i_{sqi}^m) & 0 \\ 0 & 0 & 0 \end{bmatrix}$$

$$Q_{i21}^0=\begin{bmatrix} -\dfrac{L_{mdi}}{2L_{sqi}}(\omega_i^M+\omega_i^m) & -\dfrac{L_{sdi}}{2L_{sqi}}(\omega_i^M+\omega_i^m) & 0 \\ \dfrac{n_{pi}^2}{2J_i}L_{mi}(i_{sqi}^M+i_{sqi}^m) & q_{52}^{i0} & 0 \\ 0 & 0 & 0 \end{bmatrix}$$

$$Q_{i22}^0=\begin{bmatrix} 0 & q_{54}^{i0} & 0 \\ q_{54}^{i0} & 0 & 0 \\ 0 & 0 & 0 \end{bmatrix},$$

$$q_{45}^{i0}=-\frac{1}{2}\left\{\frac{L_{mdi}}{L_{sdi}}(i_{fi}^M+i_{fi}^m)+\frac{L_{sdi}}{L_{sqi}}(i_{di}^M+i_{di}^m)\right\},$$

$$q_{52}^{i0}=\frac{n_{pi}^2}{2J_i}(L_{mdi}-L_{mqi})(i_{sqi}^M+i_{sqi}^m)$$

$$q_{54}^{i0}=\frac{n_{pi}^2}{2J_i}(L_{mi}(i_{fi}^M+i_{fi}^m)+(L_{mdi}-L_{mqi})(i_{sdi}^M+i_{sdi}^m))$$

$$\Delta Q_i=[\Delta q_{ij}^i]_{6\times6}=\begin{bmatrix} Q_{i11} & \dfrac{L_{sqi}}{2\sigma_i L_{sdi}}Q_{i12} \\ Q_{i21} & Q_{i22} \end{bmatrix}$$

$$\Delta Q_{i11}=0_{3\times3}$$

$$\Delta Q_{i12}=\begin{bmatrix} \dfrac{L_{mdi}}{L_{si}}(\omega_i^M-\omega_i^m) & \dfrac{L_{mdi}}{L_{si}}(i_{sqi}^M-i_{sqi}^m) & 0 \\ \omega_i^M-\omega_i^m & i_{sqi}^M-i_{sqi}^m & 0 \\ 0 & 0 & 0 \end{bmatrix}$$

$$\Delta Q_{i21}=\begin{bmatrix} \dfrac{L_{mdi}}{2L_{sqi}}(\omega_i^M-\omega_i^m) & \dfrac{L_{sdi}}{2L_{sqi}}(\omega_i^M-\omega_i^m) & 0 \\ \dfrac{n_{pi}^2}{2J_i}L_{mi}(i_{sqi}^M-i_{sqi}^m) & \Delta q_{52}^i & 0 \\ 0 & 0 & 0 \end{bmatrix}$$

$$\Delta Q_{i22}=\begin{bmatrix} 0 & q_{54}^{i0} & 0 \\ q_{54}^{i0} & 0 & 0 \\ 0 & 0 & 0 \end{bmatrix}$$

$$\Delta q_{45}^i=\frac{1}{2}\left\{\frac{L_{mdi}}{L_{sdi}}(i_{fi}^M-i_{fi}^m)+\frac{L_{sdi}}{L_{sqi}}(i_{di}^M-i_{di}^m)\right\},$$

$$\Delta q_{52}^i=\frac{n_{pi}^2}{2J_i}\,|\,L_{mdi}-L_{mqi}\,|\,(i_{sqi}^M-i_{sqi}^m)$$

$$\Delta q_{54}^i=\frac{n_{pi}^2}{2J_i}(L_{mi}(i_{fi}^M-i_{fi}^m)+|\,L_{mdi}-L_{mqi}\,|\,(i_{sdi}^M-i_{sdi}^m))$$

Theorem 1. For system (9), each EESM can track its own desired speed and maintain a good coordination with other motors under controller $U=KX$ if there exist a symmetric and positive-definite matrix $P1\in R^{6n\times6n}$, matrix $K\in R^{3n\times6n}$, and positive scalar λ such that the following BMI holds:

$$\begin{bmatrix} A^TP_1+P_1A+K^TB^TP_1+P_1BK+Q_0^TP_1+P_1Q_0+\lambda G_1^TG_1 & P_1E_1 \\ E_1^TP_1 & -\lambda I \end{bmatrix}<0, \tag{10}$$

Proof:

As robust control law is designed as $U=KX$, (9) is rewritten as

$$\dot{X}=(A+BK)X+F(x_j^i). \tag{11}$$

Let

$$W(x_j^i)=(A+BK)X+F(x_j^i).$$

$W(x_j^i)$ is continuously differentiable with regard to x_j^i; hence, the equation $W(x_j^i)=0$ offers a unique solution under condition (4). Assume that X_0 is the solution of equation $W(x_j^i)=0$, that is, $\dot{X}_{X=X_0}=0$. Let

$$Z=(A+BK)X+F(x_j^i) \tag{12}$$

Then, $Z=0$ when $X=X_0$. According to (11) and (12), the following equation is obtained.

$$\dot{Z}=(A+BK+Q(x_j^i))Z \tag{13}$$

where $Q(x_j^i)=diag\{Q_1\cdots Q_i\cdots Q_n\}$,

$$Q_i = \begin{bmatrix} 0 & 0 & 0 & -\dfrac{L_{mi}}{\sigma_i L_{si}}\omega_i & -\dfrac{L_{mi}}{\sigma_i L_{si}} i_{sqi} & 0 \\ 0 & 0 & 0 & -\dfrac{1}{\sigma_i}\omega_i & -\dfrac{1}{\sigma_i} i_{sqi} & 0 \\ 0 & 0 & 0 & 0 & 0 & 0 \\ -\dfrac{L_{mi}}{L_{si}}\omega_i & -\omega_i & 0 & 0 & q_i^{45} & 0 \\ \dfrac{n_{pi}^2}{J_i} L_{mi} i_{sqi} & 0 & 0 & \dfrac{n_{pi}^2}{J_i} L_{mi} i_{fi} & 0 & 0 \\ 0 & 0 & 0 & 0 & 0 & 0 \end{bmatrix}$$

$$q_i^{45} = -(\frac{L_{mi}}{L_{si}} i_{fi} + i_{sdi}).$$

A Lyapunov function is chosen as

$$V_{c1} = Z^T P_1 Z \tag{14}$$

According to Lemma 1, $Q(x_j^i)$ can be rewritten as

$$Q(x_j^i) = Q_0 + E_1 \Delta G_1, \Delta \in \Delta^* \tag{15}$$

where

$\Delta^* = \{\Delta \in R^{(5n)^2 \times (5n)^2} \mid \Delta = diag\{\chi_{11} \quad \cdots \quad \chi_{15n} \quad \cdots \quad \chi_{5n1} \quad \cdots \quad \chi_{5n5n}\},$ $\left|\chi_{ij}\right| \le 1, i, j = 1, \cdots, 5n\}.$

The following equality is obtained via (13), (14), and (15).

$$\dot{V}_{c1} = Z^T (A^T P_1 + P_1 A + K^T B^T P_1 + P_1 BK + Q_0^T P_1 + P_1 Q_0) Z \\ + Z^T G_1^T \Delta^T E_1^T P_1 Z + Z^T P_1 E_1 \Delta G_1 Z.$$

According to Lemma 3 and $\Delta^T \Delta \le I$, inequation (16) is obtained.

$$\dot{V}_{c1} \le Z^T (A^T P_1 + P_1 A + K^T B^T P_1 + P_1 BK + Q_0^T P_1 + P_1 Q_0 \\ + \lambda G_1^T G_1 + \frac{P_1 E_1 E_1^T P_1}{\lambda}) Z \tag{16}$$

If

$$A^T P_1 + P_1 A + K^T B^T P_1 + P_1 BK + Q_0^T P_1 + P_1 Q_0 + \lambda G_1^T G_1 + \frac{P_1 E_1 E_1^T P_1}{\lambda} < 0 \tag{17}$$

the time derivative of the Lyapunov function V_{c1} is negative. This result indicates that the system can be stabilized by the controller, i.e., each EESM can follow its desired speed, and the system remains coordinated. According to Schur complement theory, (17) can be rewritten as (10). This completes the proof of Theorem 1.

Remark 1. The proposed controller is $U = KX$, where $k \in R^{3n \times 6n}$; thus, matrix K can be expressed as

$$K = [k_{ij}], k_{ij} \in R^{3 \times 6}, i, j = 1, 2, ..., n.$$

In this expression, k_{ij} is the feedback gain of motor j to motor i and k_{ii} is the self-feedback gain of motor i. As each motor must track its own desired speed, $k_{ii} \ne 0$ for $i = 1, 2, ...n.$

If $k_{ij} = 0$, then the signals of the state variables of motor j are not sent to motor i, in which case motor i is not influenced by motor j. If $k_{ij} = 0$ when $i \ne j$, each motor only tracks its own desired speed without coordinating with the other motors. If every motor tracks its own desired speed and considers its coordination with other motors, then $k_{ij} \ne 0$ for all $i, j = 1, 2, ..., n$. If motor i only considers the coordination with motor j, then let $k_{ij} \ne 0$ and $k_{il} = 0$ with $l \ne i, j$.

Take three motors as an example. Motors 1 and 2 ,motors 2 and 3 should achieve good coordination performance. Thus, we should let $k_{13} = 0$, $k_{31} = 0$, $k_{12} \ne 0$, $k_{21} \ne 0$, $k_{23} \ne 0$, $k_{32} \ne 0$, and $k_{ii} \ne 0$ with $i = 1, 2, 3$.

If the cross feedback signals are enhanced in the proposed controller, the coordination performance consequently improves. As the controller design is based on the dynamic model of a drive motor and the current signal is used for cross feedback, the dynamic performance of the system is improved. A detailed description of the controller is presented in Fig. 2.

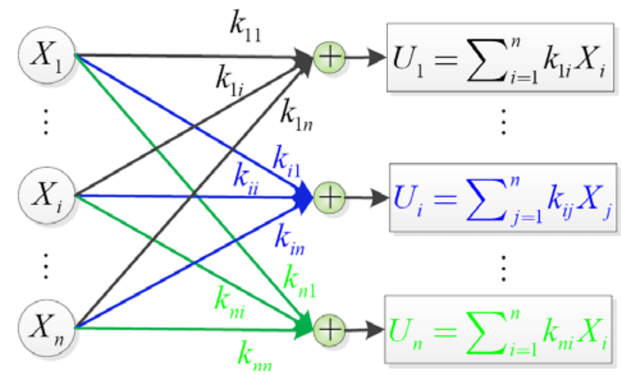

Fig. 2. Controller structure.

Remark 2. The model error and disturbance are considered in the system model, thus giving the proposed control strategy strong robustness to the environment disturbance and perturbation parameters. The load information of two motors is not required in the proposed controller, which can thus deal with load uncertainty.

Ten changeable elements make up Q_i. According to Lemma 2, Q_i can be expressed as

$$Q_i = Q_i^0 + M_i \tag{18}$$

where

$M_i = e_{6i-5} f_{14}^i e_{6i-2}^T + e_{6i-5} f_{15}^i e_{6i-1}^T + e_{6i-4} f_{24}^i e_{6i-2}^T + e_{6i-4} f_{25}^i e_{6i-1}^T + e_{6i-2}$
$\times f_{41}^i e_{6i-5}^T + e_{6i-2} f_{42}^i e_{6i-4}^T + e_{6i-2} f_{45}^i e_{6i-1}^T$
$+ e_{6i-1} f_{51}^i e_{6i-5}^T + e_{6i-1} f_{52}^i e_{6i-4}^T + e_{6i-1} f_{54}^i e_{6i-2}^T,$

with $|f_{14}^i| \le \Delta q_{14}^i$, $|f_{15}^i| \le \Delta q_{15}^i$, $|f_{24}^i| \le \Delta q_{24}^i$, $|f_{25}^i| \le \Delta q_{25}^i$, $|f_{41}^i| \le \Delta q_{41}^i$, $|f_{42}^i| \le \Delta q_{42}^i$, $|f_{45}^i| \le \Delta q_{45}^i$, $|f_{51}^i| \le \Delta q_{51}^i$, $|f_{52}^i| \le \Delta q_{52}^i$ and $|f_{54}^i| \le \Delta q_{54}^i$.

Equation (19) is obtained by combining $Q(x_j^i)$ and (11).

$$Q(x_j^i) = Q_0 + M_1 + \cdots + M_i + \cdots + M_n \tag{19}$$

Theorem 2. For system (9), each EESM can track its desired speed and maintain coordination performance with other motors if there exist a symmetric and positive-definite matrix $P_2 \in R^{5n\times 5n}$, matrix $K = \in R^{3n\times 6n}$, and real scalar $\lambda_{14}^i > 0$, $\lambda_{15}^i > 0$, $\lambda_{24}^i > 0$, $\lambda_{25}^i > 0$, $\lambda_{41}^i > 0$, $\lambda_{42}^i > 0$, $\lambda_{45}^i > 0$, $\lambda_{51}^i > 0$, $\lambda_{52}^i > 0$, and $\lambda_{54}^i > 0 (i = 1, \cdots n)$ such that the following BMI holds:

$$\begin{bmatrix} A^T P_2 + P_2 A + K^T B^T P_2 + P_2 BK + Q_0^T P_2 + P_2 Q_0 + \Upsilon_1 & \Upsilon_2 \\ \Upsilon_2^T & -\Upsilon_3 \end{bmatrix} < 0 \tag{20}$$

where

$$\begin{aligned}\Upsilon_1 = &\{\lambda_{41}^1(\Delta q_{41}^1)^2 + \lambda_{51}^1(\Delta q_{51}^1)^2\}e_1 e_1^T \\ &+ \{\lambda_{12}^1(\Delta q_{12}^1)^2 + \lambda_{52}^1(\Delta q_{52}^1)^2\}e_2 e_2^T \\ &+ \{\lambda_{14}^1(\Delta q_{14}^1)^2 + \lambda_{24}^1(\Delta q_{24}^1) + \lambda_{54}^1(\Delta q_{54}^1)^2\}e_4 e_4^T \\ &+ \{\lambda_{15}^1(\Delta q_{15}^1)^2 + \lambda_{25}^1(\Delta q_{25}^1) + \lambda_{45}^1(\Delta q_{45}^1)^2\}e_5 e_5^T \\ &+ \cdots + \{\lambda_{41}^i(\Delta q_{41}^i)^2 + \lambda_{51}^i(\Delta q_{51}^i)^2\}e_{6i-5} e_{6i-5}^T \\ &+ \{\lambda_{12}^i(\Delta q_{12}^i)^2 + \lambda_{52}^i(\Delta q_{52}^i)^2\}e_{6i-4} e_{6i-4}^T \\ &+ \{\lambda_{14}^i(\Delta q_{14}^i)^2 + \lambda_{24}^i(\Delta q_{24}^i) + \lambda_{54}^i(\Delta q_{54}^i)^2\}e_{6i-2} e_{6i-2}^T \\ &+ \{\lambda_{15}^i(\Delta q_{15}^i)^2 + \lambda_{25}^i(\Delta q_{25}^i) + \lambda_{45}^i(\Delta q_{45}^i)^2\}e_{6i-1} e_{6i-1}^T \\ &+ \cdots + \{\lambda_{41}^n(\Delta q_{41}^n)^2 + \lambda_{51}^n(\Delta q_{51}^n)^2\}e_{6n-5} e_{6n-5}^T \\ &+ \{\lambda_{12}^n(\Delta q_{12}^n)^2 + \lambda_{52}^n(\Delta q_{52}^n)^2\}e_{6n-4} e_{6n-4}^T \\ &+ \{\lambda_{14}^n(\Delta q_{14}^n)^2 + \lambda_{24}^n(\Delta q_{24}^n) + \lambda_{54}^n(\Delta q_{54}^n)^2\}e_{6n-2} e_{6n-2}^T \\ &+ \{\lambda_{15}^n(\Delta q_{15}^n)^2 + \lambda_{25}^n(\Delta q_{25}^n) + \lambda_{45}^n(\Delta q_{45}^n)^2\}e_{6n-1} e_{6n-1}^T.\end{aligned}$$

$$\begin{aligned}\Upsilon_2 = [&P_2e_1 \quad P_2e_1 \quad P_2e_2 \quad P_2e_2 \quad P_2e_4 \quad P_2e_4 \quad P_2e_4 \quad P_2e_5 \quad P_2e_5 \\ &P_2e_5 \quad \cdots \quad P_2e_{6i-5} \quad P_2e_{6i-5} \quad P_2e_{6i-4} \quad P_2e_{6i-4} \quad P_2e_{6i-2} \\ &P_2e_{6i-2} \quad P_2e_{6i-2} \quad P_2e_{6i-1} \quad P_2e_{6i-1} \quad P_2e_{6i-1} \quad \cdots \quad P_2e_{6n-5} \quad P_2e_{6n-5} \\ &P_2e_{6n-4} \quad P_2e_{6n-4} \quad P_2e_{6n-2} \quad P_2e_{6n-2} \quad P_2e_{6n-2} \quad P_2e_{6n-1} \quad P_2e_{6n-1} \quad P_2e_{6n-1}]\end{aligned}$$

$$\begin{aligned}\Upsilon_3 = diag\{&\lambda_{14}^1 \quad \lambda_{15}^1 \quad \lambda_{24}^1 \quad \lambda_{25}^1 \quad \lambda_{41}^1 \quad \lambda_{42}^1 \quad \lambda_{45}^1 \quad \lambda_{51}^1 \quad \lambda_{54}^1 \quad \cdots \\ &\lambda_{14}^i \quad \lambda_{15}^i \quad \lambda_{24}^i \quad \lambda_{25}^i \quad \lambda_{41}^i \quad \lambda_{42}^i \quad \lambda_{45}^i \quad \lambda_{51}^i \quad \lambda_{54}^i \quad \cdots \\ &\lambda_{14}^n \quad \lambda_{15}^n \quad \lambda_{24}^n \quad \lambda_{25}^n \quad \lambda_{41}^n \quad \lambda_{42}^n \quad \lambda_{45}^n \quad \lambda_{51}^n \quad \lambda_{52}^n \quad \lambda_{54}^n\}.\end{aligned}$$

Proof: The Lyapunov function is chosen as

$$V_{c2} = Z^T P_{c2} Z \tag{21}$$

On the basis of (13), (19), and (21), the following equation is obtained.

$$\begin{aligned}\dot{V}_{c2} = &Z^T(A^T P_2 + P_2 A + K^T B^T P_2 + P_2 BK + Q_0^T P_2 + P_2 Q_0)Z \\ &+ 2Z^T(e_1 f_{14}^1 e_4^T + e_1 f_{15}^1 e_5^T + e_2 f_{24}^1 e_4^T + e_2 f_{25}^1 e_5^T \\ &+ e_4 f_{41}^1 e_1^T + e_4 f_{42}^1 e_2^T + e_4 f_{45}^1 e_5^T + e_5 f_{51}^1 e_1^T + e_5 f_{54}^1 e_4^T \\ &+ \cdots + e_{6i-5} f_{14}^i e_{6i-2}^T + e_{6i-5} f_{15}^i e_{6i-1}^T + e_{6i-4} f_{24}^i e_{6i-2}^T + e_{6i-4} f_{25}^i e_{6i-1}^T \\ &+ e_{6i-2} f_{41}^i e_{6i-5}^T + e_{6i-2} f_{42}^i e_{6i-4}^T + e_{6i-2} f_{45}^i e_{6i-1}^T + e_{6i-1} f_{51}^i e_{6i-5}^T \\ &+ e_{6i-1} f_{54}^i e_{6i-2}^T + \cdots + e_{6n-5} f_{14}^n e_{6n-2}^T + e_{6n-5} f_{15}^n e_{6n-1}^T \\ &+ e_{6n-4} f_{24}^n e_{6n-2}^T + e_{6n-4} f_{25}^n e_{6n-1}^T + e_{6n-2} f_{41}^n e_{6n-5}^T \\ &+ e_{6n-2} f_{42}^n e_{6n-4}^T + e_{6n-2} f_{45}^n e_{6n-1}^T \\ &+ e_{6n-1} f_{51}^n e_{6n-5}^T + e_{6n-1} f_{54}^n e_{6n-2}^T)^T P_2 Z\end{aligned} \tag{22}$$

The following inequality is obtained via Lemma 3 and $|f_{ij}^i| \le \Delta q_{ij}^i$.

$$\dot{V}_{c1} \le Z^T M Z \tag{23}$$

where

$$\begin{aligned}M = &A^T P_2 + P_2 A + K^T B^T P_2 + P_2 BK + Q_0^T P_2 + P_2 Q_0 \\ &+ \Upsilon_1 + \frac{P_2 e_1 e_1^T P_2}{\lambda_{14}^1} + \frac{P_2 e_1 e_1^T P_2}{\lambda_{15}^1} + \frac{P_2 e_2 e_2^T P_2}{\lambda_{24}^1} + \frac{P_2 e_2 e_2^T P_2}{\lambda_{25}^1} \\ &+ \frac{P_2 e_4 e_4^T P_2}{\lambda_{41}^1} + \frac{P_2 e_4 e_4^T P_2}{\lambda_{42}^1} + \frac{P_2 e_4 e_4^T P_2}{\lambda_{45}^1} + \frac{P_2 e_5 e_5^T P_2}{\lambda_{51}^1} \\ &+ \frac{P_2 e_5 e_5^T P_2}{\lambda_{54}^1} + \cdots + \frac{P_2 e_{6i-5} e_{6i-5}^T P_2}{\lambda_{14}^i} + \frac{P_2 e_{6i-5} e_{6i-5}^T P_2}{\lambda_{15}^i} \\ &+ \frac{P_2 e_{6i-4} e_{6i-4}^T P_2}{\lambda_{24}^i} + \frac{P_2 e_{6i-4} e_{6i-4}^T P_2}{\lambda_{25}^i} + \frac{P_2 e_{6i-2} e_{6i-2}^T P_2}{\lambda_{41}^i} \\ &+ \frac{P_2 e_{6i-2} e_{6i-2}^T P_2}{\lambda_{42}^i} + \frac{P_2 e_{6i-2} e_{6i-2}^T P_2}{\lambda_{45}^i} + \frac{P_2 e_{6i-1} e_{6i-1}^T P_2}{\lambda_{51}^i} \\ &+ \frac{P_2 e_{6i-1} e_{6i-1}^T P_2}{\lambda_{54}^i} + \cdots + \frac{P_2 e_{6n-5} e_{6n-5}^T P_2}{\lambda_{14}^n} + \frac{P_2 e_{6n-5} e_{6n-5}^T P_2}{\lambda_{14}^n} \\ &+ \frac{P_2 e_{6n-4} e_{6n-4}^T P_2}{\lambda_{24}^n} + \frac{P_2 e_{6n-4} e_{6n-4}^T P_2}{\lambda_{25}^n} + \frac{P_2 e_{6n-2} e_{6n-2}^T P_2}{\lambda_{41}^n} \\ &+ \frac{P_2 e_{6n-2} e_{6n-2}^T P_2}{\lambda_{42}^n} + \frac{P_2 e_{6n-2} e_{6n-2}^T P_2}{\lambda_{45}^n} \\ &+ \frac{P_2 e_{6n-1} e_{6n-1}^T P_2}{\lambda_{51}^n} + \frac{P_2 e_{6n-1} e_{6n-1}^T P_2}{\lambda_{54}^n}.\end{aligned}$$

If $M < 0$, then the time derivative of the Lyapunov function V_{c2} is negative. This outcome indicates that each EESM can follow its desired speed and that the system can remain coordinated. $M < 0$ can be rewritten as (20) via Schur complement theory. Doing so completes the proof of Theorem 2.

IV. APPLICATION IN HIGH-POWER METAL-ROLLING SYSTEM

The proposed coordination controller is utilized for an aluminum-rolling line in a Chinese factory. Fig. 3 shows the structure of the metal-rolling system. This system comprises an inverter and an rectifier, both of which make up a typical three-level NPC topology. The transformer converts the 10 kV AC into 3 kV AC, and DC voltage is obtained via the PWM rectifier. The converter for field winding is used to control the field winding current of the EMSM. Two inverters arranged in parallel are used to control two 5 MW EESMs (Fig. 4). The parameters of the EESMs are shown in Table I. Each EESM can achieve up to 10 MW in a short time.

EESMs 1 and 2 respectively drive the up roller and the down roller to realize metal rolling. In the working process, the loads of the two EESMs often change rapidly when the metal touches the roller. The loads of the two EESMs are also different for numerous reasons, one of which is the shape of the metal, which further results in different output torques between the two motors. To achieve high-precision metal-rolling, the speeds of the two EESMs must be the same, and

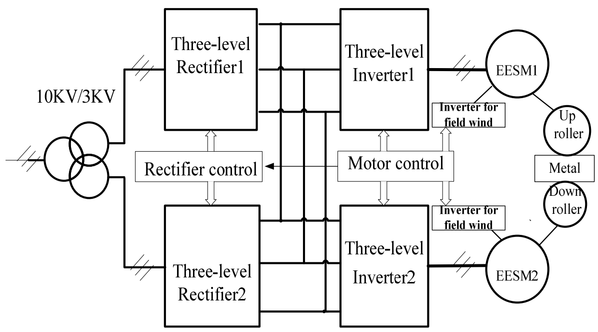

Fig. 3. Structure of metal-rolling system.

Fig. 4. Metal-rolling system with two EESMs.

TABLE I

PARAMETERS OF EESM

Rated Power	5000 kW	Rated voltage	3050 V
Rated current	982 A	Rated Speed	30 r/min
n_p	20p	R_s	0.0583 Ω
L_f	0.0628H	L_s	0.0083H
L_{md}	0.0457H	L_{mq}	0.0285H
L_{sd}	0.0540H	L_{sq}	0.0368H

the speed drop should be minimal. These goals are feasible if the proposed coordination controller is adopted.

The circuit of a three-level diode clamp inverter based on IGCT is shown in Fig. 5. The output voltage state is defined in Table II. Considering the motor parameters, we can obtain the following control parameters by solving the inequality (10) via MATLAB.

LAB soft

$$k=\left[\begin{array}{cccccccccccc} -6 & -0.4 & 0 & -0.7 & -0.1 & 0 & -0.5 & -0.1 & 0 & -0.2 & 0 & 0\\ 0 & -15 & -6 & 0 & 0 & 0 & 0 & 0 & 0 & 0 & 0 & 0\\ -0.5 & 0 & 0 & -5 & -25 & -55 & 0 & 0 & 0 & 3 & 10 & 25\\ -0.3 & -0.1 & 0 & -0.25 & 0 & 0 & -5 & -0.5 & 0 & -0.8 & -0.2 & 0\\ 0 & 0 & 0 & 0 & 0 & 0 & 0 & -20 & -8 & 0 & 0 & 0\\ 0 & 0 & 0 & 4 & 13 & 30 & 0 & 0 & 0 & -6 & -30 & -60 \end{array}\right] \tag{24}$$

Next, a simulation and an experiment are conducted to verify the effectiveness of the proposed control algorithm.

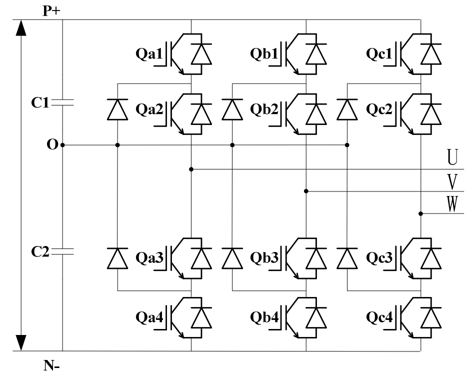

Fig. 5. Main circuit topology for three-level diode clamp inverter.

TABLE II

SWITCH STATES FOR THREE-LEVEL IGCT

Case	Phase voltage	Switch States
1	Ud/2(P)	Qa1=on,Qa2=on,Qa3=off,Qa2=off
2	0	Qa1=off,Qa2=on,Qa3=on,Qa2=off
3	Ud/2(N)	Qa1=off,Qa2=on,Qa3=on,Qa2=off

A. Simulation

The simulation is conducted in MATLAB with varying loads (T_l) and parameters (L_{md}) for the two motors.

$$T_{l,1}=T_{rated}\ ,T_{l,2}=1.2\times T_{rated}\ ,L_{md,1}=L_{md}\ ,L_{md,2}=1.2\times L_{md} \tag{25}$$

The desired speed of the two motors is 27 r/m. The load is added to the system at 2 s and removed at 3.5 s.

A comparison between the proposed method and the traditional proportional–integral (PI) controller is conducted to further demonstrate the control performance of the proposed controller. The PI speed controller is used in the outer loop, whereas the PI current controller is used in the inner loop of each motor. The PI law can be presented as

$$u_{d1}=k_{Pi_{d1}}i_{d1}+k_{Ii_{d1}}\int_0^t i_{d1}d\tau, u_{q1}=kk_{P\tilde{i}_{d1}}\tilde{i}_{d1}+k_{I\tilde{i}_{d1}}\int_0^t \tilde{i}_{d1}d\tau$$

$$u_{d2}=k_{Pi_{d2}}i_{d2}+k_{Ii_{d2}}\int_0^t i_{d2}d\tau, u_{q2}=kk_{P\tilde{i}_{d2}}\tilde{i}_{d2}+k_{I\tilde{i}_{d2}}\int_0^t \tilde{i}_{d2}d\tau$$

where $\tilde{i}_{q1}=i_{q1}-i_{q1}^*$, $\tilde{i}_{q2}=i_{q2}-i_{q2}^*$, $\tilde{\omega}_1=\omega_1-\omega^*$, $\tilde{\omega}_2=\omega_2-\omega^*$.

The control gains of all controllers shown below are elaborately selected to obtain optimal synchronization and tracking performance.

$$k_{Pi_{d1}}=-120, k_{Ii_{d1}}=-50, k_{P\omega 1}=-1.4,$$

$$k_{Ii_{\omega 1}}=-30, k_{P\tilde{i}_{q1}}=-13, k_{I\tilde{i}q1}=-2,$$

$$k_{Pi_{d2}}=-140, k_{Ii_{d2}}=-60, k_{P\omega_2}=-0.7,$$

$$k_{I\omega_2}=-25, k_{P\tilde{i}_{q2}}=-8, k_{I\tilde{i}_{q2}}=-1.5$$

The control performance of a traditional PI controller is depicted in Fig. 6, which shows the speed error at maximal (0.36 r/m) when the load is changed. Fig. 7 shows the results achieved with the proposed controller. The maximal speed

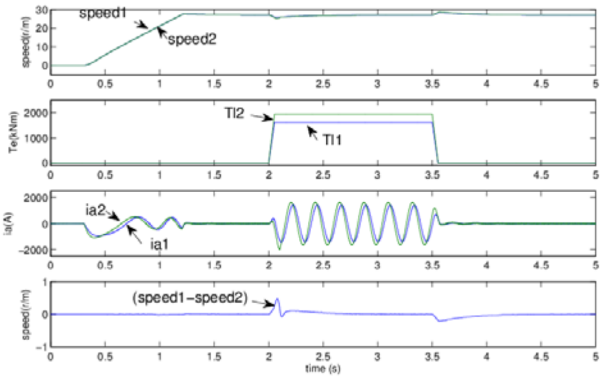

Fig. 6. Performance of traditional PI controller.

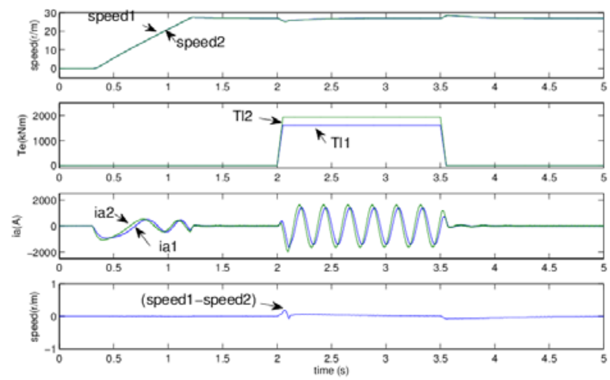

Fig. 7. Performance of proposed controller.

error is 0.11 r/m, which proves the effectiveness of the proposed method when the parameters and loads of the two motors are different (25). This result also indicates that the proposed controller exhibits a superior performance relative to the traditional PI controller. Note that the load information of two motors is not required in the proposed controller and that the proposed controller can deal with load uncertainty.

B. Experiment

The proposed coordination controller is then used in the metal-rolling system of Guangxi Liuzhou Yinhai Aluminium Co., Ltd., and the experimental data are recorded with a specific software program. Fig. 8 shows the results achieved with the proposed algorithm without load. The results indicate that regardless of whether the system is in steady state or dynamic state, the speed error between the motors is nearly zero.

Fig. 9 shows the results obtained with the proposed algorithm under the rolling condition. When the roller touches the metal, the maximum speed error between the motors is less than 0.7 rpm, and the error converges to nearly zero in a short time. This result demonstrates the good control performance of the proposed controller. Similarly, the load information of two motors is not required in the proposed controller, which can thus deal with load uncertainty. Fig. 10 shows the production of an aluminum strip and reveals the successful use of the proposed controller in the metal-rolling system.

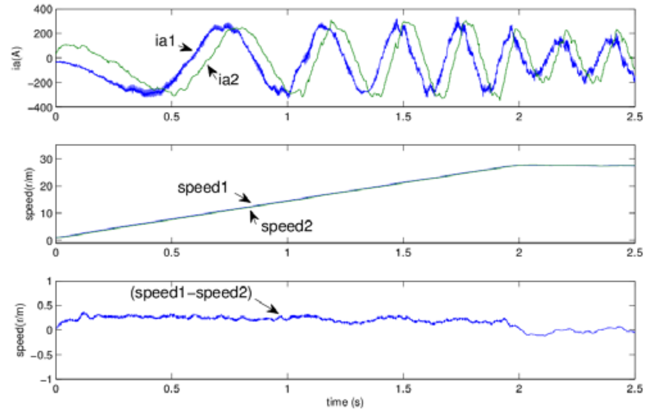

Fig. 8. Start process in no-load condition.

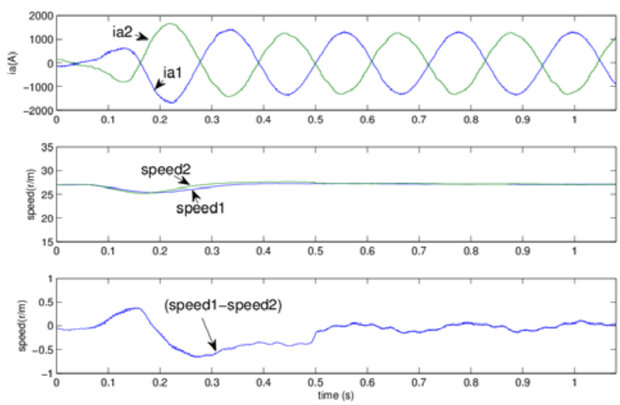

Fig. 9. Process under the rolling condition.

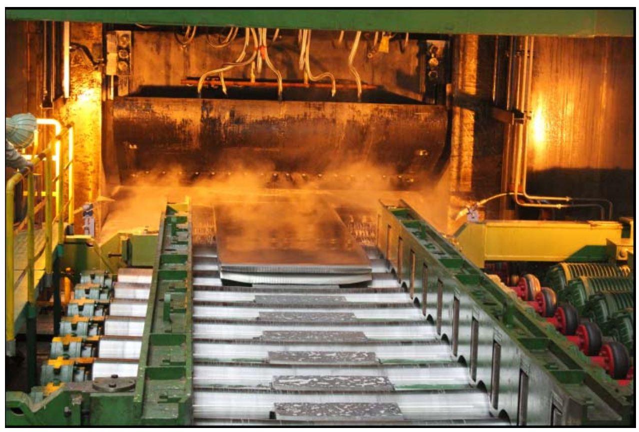

Fig. 10. Aluminum strip produced with the designed system.

V. Conclusions

This paper presents a coordination control strategy for multiple EESM systems via cross coupling and an interval matrix. The proposed controller is successfully applied in a high-power aluminum rolling system. It can deal with load uncertainty, i.e., the load information is not required in the controller. The simulation and experimental results verify the good dynamical and static performance of the proposed control strategy and its superior coordination performance relative to traditional PI controllers.

ACKNOWLEDGMENT

This paper was supported in part by the National Science Foundation of China under grants 61473314 and 61403425 and by the National Science Foundation of China through the Science Foundation of Innovation Research Group under grant 61321003.

REFERENCES

[1] Z. Zhang, K. T. Chau, and Z. Wang, "Chaotic speed synchronization control of multiple induction motors using stator flux regulation," *IEEE Trans. Magn.*, Vol. 48, No. 11, pp. 4487–4490, Nov. 2012.

[2] F.-J. Lin, P.-H. Chou, C.-S. Chen, and Y.-S. Lin, "DSP-based cross coupled synchronous control for dual linear motors via intelligent complementary sliding mode control," *IEEE Trans. Ind. Electron.*, Vol. 59, No. 2, pp. 1061–1073, Feb. 2012.

[3] D. Z. Zhao, C. W. Li, and J. Ren, "Speed synchronisation of multiple induction motors with adjacent cross-coupling control," in *Proceedings of the 48th IEEE Conference on Decision and Control*, pp. 6805–6810, Dec. 2009.

[4] K. L. Barton and A. G. Alleyne, "A cross-coupled iterative learning control design for precision motion control," *IEEE Trans. Control Syst. Technol.*, Vol. 16, No. 6, pp. 1218–1231, Nov. 2008.

[5] Y. Xiao, K. Y. Zhu, and H. C. Liaw, "Generalized synchronization control of multi-axis motion systems," *Control Engineering Practice*, Vol. 13, No. 7, pp. 809–819, Jul. 2005.

[6] Y. Xiao and K. Y. Zhu, "Optimal synchronization control of high precision motion systems," *IEEE Trans. Ind. Electron.*, Vol. 53, No. 4, pp. 1160–1169, Jun. 2006.

[7] D. Sun, "Position synchronization of multiple motion axes with adaptive coupling control," *Automatica*, Vol. 39, No. 6, pp. 997–1005, Jun. 2003.

[8] Y. C. Liu and N. Chopra, "Controlled synchronization of heterogeneous robotic manipulators in the task space," *IEEE Trans. Robot.*, Vol. 28, No. 1, pp. 268–275, Feb. 2012.

[9] H. Y. Chuang and C. H. Liu, "A model-referenced adaptive control strategy for improving contour accuracy of multiaxis machine tools," *IEEE Trans. Ind. Appl.*, Vol. 28, No. 1, pp. 221–227, Jan./Feb. 1992.

[10] J.-H. Chin, Y.-M. Cheng, and J.-H. Lin, "Improving contour accuracy by fuzzy-logic enhanced cross-coupled precompensation method," *Robotics and Computer-Integrated Manufacturing*, Vol. 20, No. 1, pp. 65–76, Feb. 2004.

[11] P. R. Moore and C. M. Chen, "Fuzzy-logic coupling and synchronized control of multiple independent servo-drives," *Control Engineering Practice*, Vol. 3, No. 12, pp. 1697–1708, Dec. 1995.

[12] M. A. Valenzuela and R. D. Lorenz, "Electronic line-shafting control for paper machine drives," *IEEE Trans. Ind. Appl.*, Vol. 37, No. 1, pp. 158–164, Jan./Feb. 2001.

[13] R. G. Anderson, A. J. Meyer, M. A. Valenzuela, and R. D. Lorenz, "Web machine coordinated motion control via electronic line-shafting," *IEEE Trans. Ind. Appl.*, Vol. 37, No. 1, pp. 247–254, Jan./Feb. 2001.

[14] C.-S. Chen and L.-Y. Chen, "Robust cross-coupling synchronous control by shaping position commands in multiaxes system," *IEEE Trans. Ind. Electron.*, Vol. 59, No. 12, pp. 4761–4773, Dec. 2012.

[15] M. H. Cheng, Y. J. Li, and E. G. Bakhoum, "Controller synthesis of tracking and synchronization for multiaxis motion system," *IEEE Trans. Control Syst. Technol.*, Vol. 22, No. 1, pp. 378–386, Jan. 2014.

[16] Y. H. Li, Q. Zheng, and L. M. Yang, "Design of robust sliding mode control with disturbance observer for multi-axis coordinated traveling system," *Computers & Mathematics with Applications*, Vol. 64, No. 5, pp.759–765, Sep. 2012.

[17] N. R. Abjadi, J. Soltani, J. Askari, and G. R. A. Markadeh, "Nonlinear sliding-mode control of a multi-motor web-winding system without tension sensor," *IET Control Theory & Applications*, Vol. 3, No. 4, pp. 419–427, Apr. 2009.

[18] D. Knittel, E. Laroche, D. Gigan, and H. Koc, "Tension control for winding systems with two-degrees-of-freedom h-infinity controllers," *IEEE Trans. Ind. Appl.*, Vol. 39, No. 1, pp. 113–120, Jan./Feb. 2003.

[19] A. Benlatreche, D. Knittel, and E. Ostertag, "Robust decentralized control strategies for large-scale web handling systems," *Control Engineering Practice*, Vol. 16, No. 6, pp. 736–750, Jun. 2008.

[20] F. J. Lin, H. J. Hsieh, Y. S. Lin, and P. H. Chou, "Digital signal processor-based cross-coupled synchronous control of dual linear motors via functional link radial basis function network," *IET Control Theory & Applications*, Vol. 5, No. 4, pp. 552–564, Mar. 2011.

[21] F. Claveau, P. Chevrel, and K. Knittel, "A 2DOF gain-scheduled controller design methodology for a multi-motor web transport system," *Control Engineering Practice*, Vol. 16, No. 5, pp. 609–622, May 2008.

[22] D. Sun, X. Y. Shao, and G. Feng, "A model-free cross-coupled control for position synchronization of multi-axis motions: theory and experiments," *IEEE Trans. Control Syst. Technol.*, Vol. 15, No. 2, pp. 306–314, Mar. 2007.

[23] L. Guo, "$H\infty$ output feedback control for delay systems with nonlinear and parametric uncertainties," *IEE Proceedings - Control Theory and Applications*, Vol. 149, No. 3, pp. 226–236, May 2002.

[24] W.-J. Mao and J. Chu, "Quadratic stability and stabilization of dynamic interval systems," *IEEE Trans. Autom. Control*, Vol. 48, No. 6, pp. 1007–1012, Jun. 2003.

[25] H. H. Choi, V. Q. Leu, Y. S. Choi, and J. W. Jung, "Adaptive speed controller design for a permanent magnet synchronous motor," *IET Electric Power Applications*, Vol. 5, No. 5, pp. 457–464, May 2011.

[26] Z. Deng, J. Shang, and X. Nian, "Synchronization controller design of two coupling permanent magnet synchronous motors system with nonlinear constraints," *ISA Transactions*, Vol. 59, pp. 243–255, Nov. 2015.

[27] Y. Z. Zhou and S. P. Long, "Sensorless direct torque control for electrically excited synchronous motor based on injecting high-frequency ripple current into rotor winding," *IEEE Trans. Energy Convers.*, Vol. 30, No. 1, pp. 246–253, Mar. 2015.

[28] X. Q. Wu, G. J. Tan, Q. Q. Zhang, and W. Jing, "Research of electrically excited synchronous motor vector control system based on full-order closed-loop air gap flux estimator," in *IEEE 6th International Power Electronics and Motion Control Conference*, pp. 2054–2056, May 2009.

[29] J.-G. Lu and Y.-Q. Chen, “Robust stability and stabilization of fractional-order interval systems with the fractional order a: The 0 < a < 1 case,” *IEEE Trans. Autom. Control*, Vol. 55, No. 1, pp. 152–158, Jan. 2010.
[30] P. P. Khargonekar, I. R. Petersen, and K. Zhou, “Robust stabilization of uncertain linear systems: quadratic stabilizability and h control theory,” *IEEE Trans. Autom. Control*, Vol. 35, No. 3, pp. 356–361, Mar. 1990.
[31] B. Chen, Y. Yuan, W. Chen, G. Ni, and M. Chen, “Electric drive automatic control system: motion control system,” *China Machine Press*, Chapter 8, the third edition, Beijing, China, 2003.

Jing Shang was born in Sichuan Province, China, in 1977. He received his B.S. degree in Mechanical Engineering and his M.S. degree in Electric System and Automation from Southwest Jiaotong University, China, in 2000 and 2003, respectively. He is currently working toward his Ph.D. degree at the School of Information Science and Engineering, Central South University, Changsha, China. His current research interests include control methods for high-power converters and optimal pulse-width modulation techniques.

Xionghong Nian was born in Gansu, China, in 1965. He received his B.S, M.S., and Ph.D. degrees from Northwest Normal University, Shandong University, and Peking University in 1985, 1996, and 1999, respectively. He was a Research Fellow in the Institute of Zhuzhou Electric Locomotive from 2004 to 2008. Currently, he is a Professor and Dean of the Faculty of Control Engineering of Central South University and an Editor of Converter Technology & Electric Traction. His research interests are coordinated control and optimization of complicated multi-agent systems, converter technology and drive control, and control of tractive power supply systems in high-speed trains.

Yong Liu was born in Hunan Province, China, in 1981. He received his B.S. degree in Mechanical Engineering from Xiangtan University in 2003 and his M.S. and Ph.D. degrees in Mechanical Engineering from Harbin Institute of Technology, China, in 2005 and 2010, respectively. Since 2010, He has been working as a Research Engineer in Zhuzhou Institute of Electric Locomotive. His current research interests include control methods for high-power converters and sensorless control of induction motors.